Supporting Information

Dual Interfacial Polarization Enhancement to Design Tunable Microwave Absorption Nanofibers of SiC@C@PPy

Chang Xu,[a] Fan Wu,*[abc] Liqun Duan,[a] Ziming Xiong,[a] Yilu Xia,[a] Zhiqian Yang,[a] Mengxiao Sun,[bc] Aming Xie*[b]

[a] State Key Laboratory for Disaster Prevention & Mitigation of Explosion & Impact, Army Engineering University of PLA, Nanjing 210007, China.

[b] School of Mechanical Engineering, Nanjing University of Science and Technology, Nanjing 210094, China.

[c] Department of Mechanical Engineering and Materials Science, Pratt School of Engineering, Duke University, Durham, North Carolina, 27708, USA.

Corresponding Authors

E-mail addresses: wufan@njust.edu.cn fan.wu160@duke.edu (Dr. Fan Wu); xieaming@njust.edu.cn (Dr. Aming Xie)

Basic electromagnetic theory

The attenuation constant (α) can be expressed as:

$$\alpha = \frac{\sqrt{2}\pi f}{c} \times \sqrt{(\mu''\varepsilon'' - \mu'\varepsilon') + \sqrt{(\mu''\varepsilon'' - \mu'\varepsilon')^2 + (\mu'\varepsilon'' + \mu''\varepsilon')^2}}$$

Where ε' and ε'' is the real part and imaginary part of relative complex permittivity (ε_r), respectively, μ' and μ'' is the real part and imaginary part of relative complex permeability (μ_r), respectively, f is the frequency, c is the velocity of EM waves in free space.

The impedance of the materials can be written as:

$$|Z| = \left|\sqrt{\frac{\mu_r}{\varepsilon_r}}\right|$$

According to the transmission line theory, the reflection loss can be expressed as:

$$Z_{in} = Z_0\sqrt{\frac{\mu_r}{\varepsilon_r}}tanh\left(j\frac{2\pi f d}{c}\sqrt{\mu_r\varepsilon_r}\right)$$

$$RL = 20log\left|\frac{Z_{in} - Z_0}{Z_{in} + Z_0}\right|$$

Where Z_{in} is the input impedance, d is the thickness, Z_0 is air impedance.

According to Debye theory and free electron theory, ε' and ε'' can be expressed as:

$$\varepsilon' = \varepsilon_\infty + \frac{\varepsilon_s - \varepsilon_\infty}{1 + (2\pi f)^2\tau^2}$$

$$\varepsilon'' = \varepsilon_p'' + \varepsilon_c'' = (\varepsilon_s - \varepsilon_\infty)\frac{2\pi f\tau}{1 + (2\pi f)^2\tau^2} + \frac{\sigma}{2\pi f\varepsilon_0}$$

Where ε_s is the stationary dielectric constant, ε_∞ is the optical dielectric constant, f is the frequency, τ is the polarization relaxation time, σ is the conductivity, ε_p'' is the polarization loss part and ε_c'' is the conductive loss part.

When the effect of conductive loss is negligible, the relationship between ε' and ε'' can be written as:

$$\left(\varepsilon' - \frac{\varepsilon_s + \varepsilon_\infty}{2}\right)^2 + (\varepsilon'')^2 = \left(\frac{\varepsilon_s - \varepsilon_\infty}{2}\right)^2$$

Generally, a hemicycle curve of ε' and ε'' which is named as Cole-Cole semicircle.

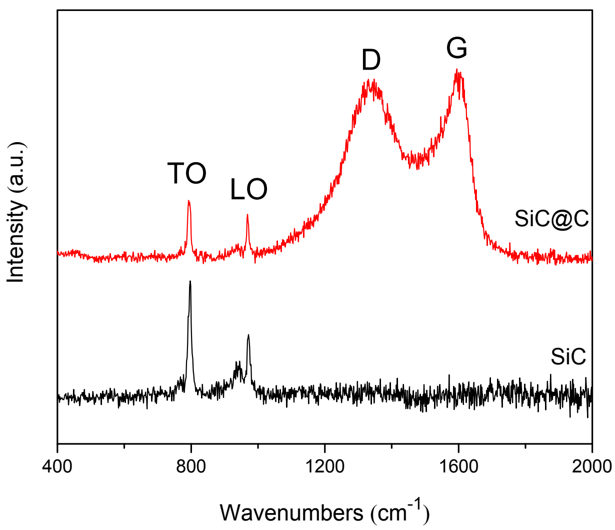

Fig. S1 Raman spectra of SiC and SiC

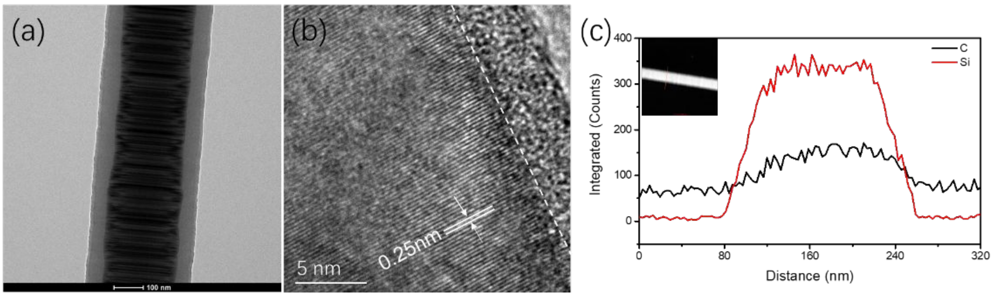

Fig. S2 (a) TEM, (b) HRTEM and (c) element line-scanning images of SiC@C

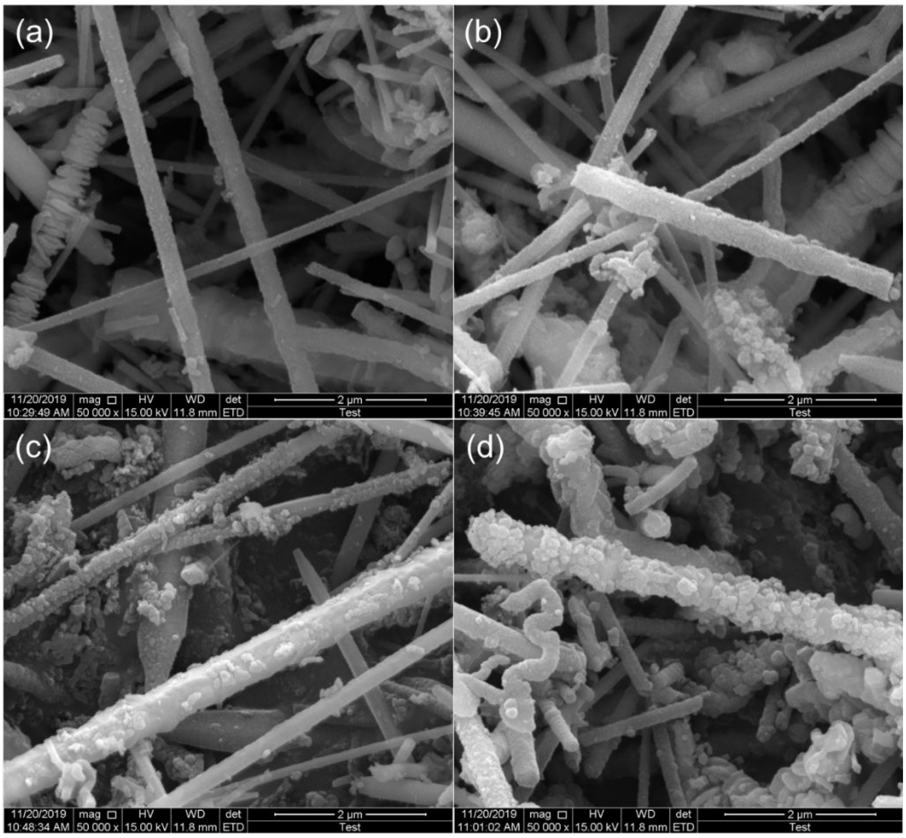

Fig. S3 SEM images of (a) SiC@C@PPy-1, (b) SiC@C@PPy-2, (c) SiC@C@PPy-3, (d) SiC@C@PPy-4.

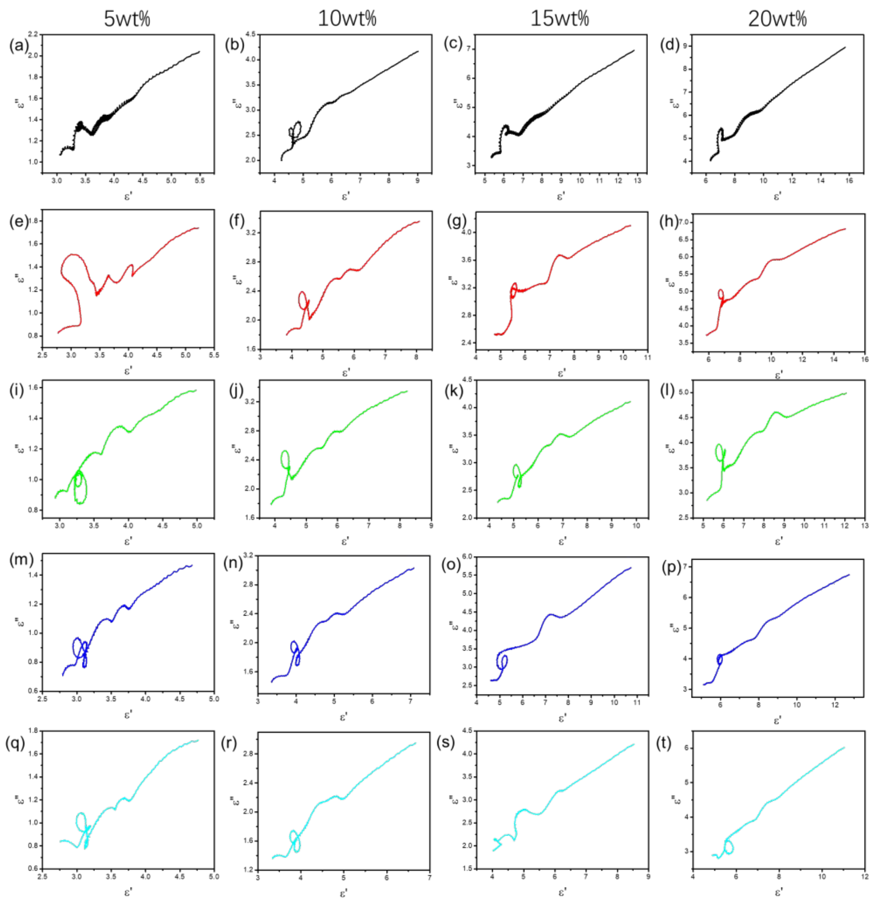

Fig. S4 Cole-Cole curves of (a-d) SiC@C, (e-h) SiC@C@PPy-1, (i-l) SiC@C@PPy-2, (m-p) SiC@C@PPy-3, (q-t) SiC@C@PPy-4.

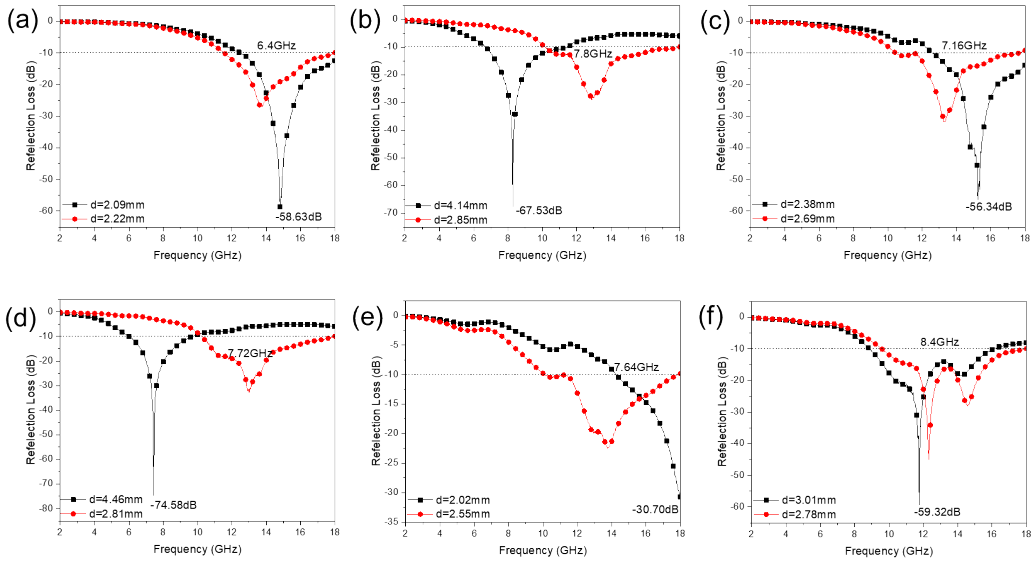

Fig. S5 The best electromagnetic absorption performance of (a) SiC, (b) SiC@C, (c) SiC@C@PPy-1, (d) SiC@C@PPy-2, (e) SiC@C@PPy-3, (f) SiC@C@PPy-4.

Table S1 The comparable of EM absorption between this work and recent reported absorber.

Samples	Minimum RL (dB)	Thickness (mm)	EAB (GHz)	Thickness (mm)	Loading ratio (wt%)	Matrix	Ref.
SiC NWs	-30.0	4.6	3.7	3.7	50	Paraffin	1
SiC powders	-16.03	2.1	3.3	2.1	-	-	2
SiC microtubes	-23.90	1.0	2.0	1.0	20	Paraffin	3
SiC ceramic	-60.00	4.0	4.0	4.0~5.0	60	Paraffin	4
Fe-doped SiC	-55.00	2.5	2.48	2.0	-	-	5
Cr-SiC	-37.08	1.7	3.02	1.7	20	epoxy	6
Mn-SiC	-43.35	1.8	3.02	1.8	20	epoxy	6
Ni-SiC	-48.06	-	4.2	-	-	-	7
Si_3N_4–SiC-1	-27.10	2.5	2.7	2.5	-	-	8
Co-SiC@C	-53.0	4.8	5.8	1.8	80	Paraffin	9
SiC@Co	-25.0	2.5	6.6	2.5	50	Paraffin	10
SiC@PPy	-19.1	2.0	6.52	2.5	10	Paraffin	11
SiC-ZnO	-42.11	3.5	6.6	2.5	10	Paraffin	12
SiCnw-CF/PPy	-50.19	2.0	6.2	2.0	30	Paraffin	13

SiC aerogels	-43.0	2.0	4.0	2.0	10	Paraffin	14
Au-SiC	-50.6	-	7.2	2.7	10	Paraffin	15
SiC@C	-59.4	2.49	7.3	2.7	30	Paraffin	16
SiC@C	-50.0	2.80	8.0	2.80	50	Paraffin	17
Ni@SiC	-42.1	2.88	7.2	3.0	60	Paraffin	18
SiCnws/GA	-63.76	1.67	4.6	2.0	30	Paraffin	19
SiCnws/GA-PPy	-59.1	2.62	5.9	1.83	30	Paraffin	19
SiCw–GNs/PPy	-64.2	-	7.6	2.02	-	Paraffin	20
SiCnw/GA-S	-54.8	3.63	6.5	2.0	20	Paraffin	21
HfC/SiC	-33.9	3.0	7.4	3.0	10	silicon resin	22
$Gd(OH)_3$@PPy	-51.4	2.2	4.8	2.2	20	Paraffin	23
CNTs@PANi	-45.7	2.4	5.6	2.0	10	Paraffin	24
$CoFe_2O_4$/RGO/$CoFe_2O_4$	-53.3	2.6	7.08	2.6	20	Paraffin	25
Co/MnO	-64.2	2.3	6.0	2.1	80	Paraffin	26
HGS@PAC	-32.43	3.70	4.2	3.50	10	-	27
Fe@C	-54.4	4.5	8.1	3.0	30	Paraffin	28
CNT@TiO_2	-31.8	2.0	2.76	2.0	30	Paraffin	29

PANI/GA	-42.3	3.0	3.2	3.0	30	Paraffin	30
PPy/ZIFs	-49	2.9	7.24	2.6	30	Paraffin	31
$Ti_3C_2T_x$/PANI	-58.3	1.8	-	-	-	Paraffin	32
CNT-Fe_3O_4-PANI	-53.2	1.8	5.87	1.8	-	Paraffin	33
Fe_3O_4/MWCNTs	-63.64	1.6	-	-	50	Paraffin	34
PVB-MnO_2	-37	2.0	-	-	5	-	35
$CoFe_2O_4$/rGO	-57.7	2.8	5.8	2.8	50	Paraffin	36
SiCnws	-58.63	2.09	6.4	2.22	15	Paraffin	This work
SiC@C	-56.34	2.38	7.16	2.69	10	Paraffin	This work
SiC@C/PPy-1	-67.53	4.14	7.8	2.85	10	Paraffin	This work
SiC@C/PPy-2	-74.58	4.46	7.72	2.81	10	Paraffin	This work
SiC@C/PPy-3	-30.70	2.02	7.64	2.55	15	Paraffin	This work
SiC@C/PPy-4	-59.32	3.01	8.4	2.78	15	Paraffin	This work

Table S2 The thinnest thicknesses for a sample can effectively attenuate the electromagnetic energy in the X and Ku band.

Sample	d_X (mm)	d_{Ku} (mm)
SiC@C/PPy-1	3.58	2.56
SiC@C/PPy-2	3.56	2.44
SiC@C/PPy-3	3.15	2.40
SiC@C/PPy-4	3.38	2.39

Reference

(1) H. Zhang, Y. Xu, J. Zhou, J. Jiao, Y. Chen, H. Wang, C. Liu, Z. Jiang, Z. Wang, Stacking fault and unoccupied densities of state dependence of electromagnetic wave absorption in SiC nanowires, *J. Mater. Chem. C* **2015**, 3, 4416–4423.

(2) H.J. Yang, J. Yuan, Y. Li, Z.L. Hou, H.B. Jin, X.Y. Fang, M.S. Cao, Silicon carbide powders: Temperature-dependent dielectric properties and enhanced microwave absorption at gigahertz range. *Solid State Commun.* **2013**, 163, 1–6.

(3) S. Meng, X. Guo, G. Jin, Y. Wang, S. Xie, Preparation and microwave absorbing properties of SiC microtubes. *J. Mater. Sci.* **2012**, 47, 2899–2902.

(4) C. Liu, D. Yu, D.W. Kirk, Y. Xu, Porous silicon carbide derived from apple fruit with high electromagnetic absorption performance. *J. Mater. Chem. C* **2016**, 4, 5349–5356.

(5) X. Su, Y. Jia, J. Wang, J. Xu, X. He, C. Fu, S. Liu, Combustion synthesis and microwave absorption property of SiC(Fe) solid solution powder under different reaction time. *J. Mater. Sci. Mater. Electron.* **2013**, 24, 1905–1912.

(6) A. Kumar, V. Agarwala, D. Singh, Effect of milling on dielectric and microwave absorption properties of SiC based composites. *Ceram. Int.* **2014**, 40, 1797–1806.

(7) J. Yuan, H.J. Yang, Z.L. Hou, W.L. Song, H. Xu, Y.Q. Kang, H.B. Jin, X.Y. Fang, M.S. Cao, Ni-decorated SiC powders: Enhanced high-temperature dielectric properties and microwave absorption performance. *Powder Technol.* **2013**, 237, 309–313.

(8) G. Zheng, X. Yin, J. Wang, M. Guo, X. Wang, Complex Permittivity and Microwave Absorbing Property of Si 3N 4-SiC Composite Ceramic. *J. Mater. Sci. Technol.* **2012**, 28, 745–750.

(9) S. Xie, X.N. Guo, G.Q. Jin, X.Y. Guo, Carbon coated Co-SiC nanocomposite with

high-performance microwave absorption. Phys. *Chem. Chem. Phys.* **2013**, 15, 16104–16110.

(10) H. Wang, L. Wu, J. Jiao, J. Zhou, Y. Xu, H. Zhang, Z. Jiang, B. Shen, Z. Wang, Covalent interaction enhanced electromagnetic wave absorption in SiC/Co hybrid nanowires. *J. Mater. Chem. A* **2015**, 3, 6517–6525.

(11) K. Zhang, M. Sun, W. Jiang, Y. Wang, D. Wang, F. Wu, A. Xie, W. Dong, A core-shell polypyrrole@silicon carbide nanowire (PPy@SiC) nanocomposite for the broadband elimination of electromagnetic pollution. *RSC Adv.* **2016**, 6, 43056–43059.

(12) M. Sun, X. Lv, A. Xie, W. Jiang, F. Wu, Growing 3D ZnO nano-crystals on 1D SiC nanowires: Enhancement of dielectric properties and excellent electromagnetic absorption performance. *J. Mater. Chem. C* **2016**, 4, 8897–8902.

(13) L. Yan, C. Hong, B. Sun, G. Zhao, Y. Cheng, S. Dong, D. Zhang, X. Zhang, In Situ Growth of Core-Sheath Heterostructural SiC Nanowire Arrays on Carbon Fibers and Enhanced Electromagnetic Wave Absorption Performance. *ACS Appl. Mater. Interfaces* **2017**, 9, 6320–6331.

(14) C. Liang, Z. Wang, Eggplant-derived SiC aerogels with high-performance electromagnetic wave absorption and thermal insulation properties. *Chem. Eng. J.* **2019**, 373, 598–605.

(15) J. Kuang, X. Hou, T. Xiao, Q. Zheng, Q. Wang, P. Jiang, W. Liu, W. Cao, Enhanced dielectric permittivity and microwave absorbing properties of Au-decorated SiC nanowires. *Jpn. J. Appl. Phys.* **2019**, 58, 060916.

(16) S. Dong, W. Zhang, X. Zhang, P. Hu, J. Han, Designable synthesis of core-shell SiCw@C heterostructures with thickness-dependent electromagnetic wave absorption between the whole X-band and Ku-band. *Chem. Eng. J.* **2018**, 354, 767–776.

(17) C. Liang, Z. Wang, Controllable Fabricating Dielectric-Dielectric SiC@C Core-Shell Nanowires for High-Performance Electromagnetic Wave Attenuation. *ACS Appl. Mater. Interfaces* **2017**, 9, 40690–40696.

(18) Z.J. Li, G.M. Shi, Q. Zhao, Improved microwave absorption properties of core–shell type Ni@SiC nanocomposites. *J. Mater. Sci. Mater. Electron.* **2017**, 28 5887–5897.

(19) Y. Cheng, P. Hu, S. Zhou, L. Yan, B. Sun, X. Zhang, W. Han, Achieving tunability of effective electromagnetic wave absorption between the whole X-band and Ku-band via adjusting PPy loading in SiC nanowires/graphene hybrid foam. *Carbon* **2018**, 132, 430–443.

(20) S. Dong, X. Zhang, W. Zhang, J. Han, P. Hu, A multiscale hierarchical architecture of a SiC whiskers-graphite nanosheets/polypyrrole ternary composite for enhanced electromagnetic wave absorption. *J. Mater. Chem. C* **2018**, 6, 10804–10814.

(21) Y. Cheng, M. Tan, P. Hu, X. Zhang, B. Sun, L. Yan, S. Zhou, W. Han, Strong and thermostable SiC nanowires/graphene aerogel with enhanced hydrophobicity and electromagnetic wave absorption property. *Appl. Surf. Sci.* **2018**, 448, 138–144.

(22) Y. Hou, L. Cheng, Y. Zhang, Y. Yang, C. Deng, Z. Yang, Q. Chen, X. Du, C. Zhao, L. Zheng, Enhanced Flexibility and Microwave Absorption Properties of HfC/SiC Nanofiber Mats. *ACS Appl. Mater. Interfaces* **2018**, 10, 29876–29883.

(23) W. Wei, X. Liu, W. Lu, H. Zhang, J. He, H. Wang, Y. Hou, Light-weight Gadolinium Hydroxide@polypyrrole Rare-Earth Nanocomposites with Tunable and Broadband Electromagnetic Wave Absorption. *ACS Appl. Mater. Interfaces* **2019**, 11, 12752–12760.

(24) H. Wang, F. Meng, F. Huang, C. Jing, Y. Li, W. Wei, Z. Zhou, Interface Modulating CNTs@PANi Hybrids by Controlled Unzipping of the Walls of CNTs to Achieve Tunable High-Performance Microwave Absorption. *ACS Appl. Mater. Interfaces* **2019**, 11, 12142–12153.

(25) K. Zhang, J. Li, F. Wu, M. Sun, Y. Xia, A. Xie, Sandwich CoFe2O4/RGO/CoFe2O4 Nanostructures for High-Performance Electromagnetic Absorption. *ACS Appl. Nano Mater.* **2019**, 2, 315–324.

(26) D. Xu, J. Qiao, N. Wu, W. Liu, F. Wang, L. Lv, J. Pan, Y. Dong, J. Liu, Facile Synthesis of Three-Dimensional Porous Co/MnO Composites Derived from Bimetal Oxides for Highly Efficient Electromagnetic Wave Absorption. *ACS Sustain. Chem. Eng.* **2019**, 7, 8687–8695.

(27) H. Xu, X. Yin, M. Zhu, M. Li, H. Zhang, H. Wei, L. Zhang, L. Cheng, Constructing hollow graphene nano-spheres confined in porous amorphous carbon particles for

achieving full X band microwave absorption. *Carbon* **2019**, 142, 346–353.
(28) X.P. Li, Z. Deng, Y. Li, H. Bin Zhang, S. Zhao, Y. Zhang, X.Y. Wu, Z.Z. Yu, Controllable synthesis of hollow microspheres with Fe@Carbon dual-shells for broad bandwidth microwave absorption. *Carbon* **2019**, 147, 172–181.
(29) Z. Mo, R. Yang, D. Lu, L. Yang, Q. Hu, H. Li, H. Zhu, Z. Tang, X. Gui, Lightweight, three-dimensional carbon Nanotube@TiO2 sponge with enhanced microwave absorption performance. *Carbon* **2019**, 144, 433–439.
(30) Y. Wang, X. Gao, Y. Fu, X. Wu, Q. Wang, W. Zhang, C. Luo, Enhanced microwave absorption performances of polyaniline/graphene aerogel by covalent bonding. *Compos. Part B Eng.* **2019**, 169, 221–228.
(31) Y. Jiao, J. Li, A. Xie, F. Wu, K. Zhang, W. Dong, X. Zhu, Confined polymerization strategy to construct polypyrrole/zeolitic imidazolate frameworks (PPy/ZIFs) nanocomposites for tunable electrical conductivity and excellent electromagnetic absorption. *Compos. Sci. Technol.* **2019**, 174, 232–240.
(32) H. Wei, J. Dong, X. Fang, W. Zheng, Y. Sun, Y. Qian, Z. Jiang, Y. Huang, Ti3C2Tx MXene/polyaniline (PANI) sandwich intercalation structure composites constructed for microwave absorption. *Compos. Sci. Technol.* **2019**, 169 52–59.
(33) J. Li, Y. Duan, W. Lu, T.W. Chou, Polyaniline-stabilized electromagnetic wave absorption composites of reduced graphene oxide on magnetic carbon nanotube film. *Nanotechnology* **2018**, 29, 155201.
(34) K. Yu, M. Zeng, Y. Yin, X. Zeng, J. Liu, Y. Li, W. Tang, Y. Wang, J. An, J. He, R. Yu, MWCNTs as Conductive Network for Monodispersed Fe3O4 Nanoparticles to Enhance the Wave Absorption Performances. *Adv. Eng. Mater.* 2018, 20, 1–8.
(35) P.J. Bora, I. Azeem, K.J. Vinoy, P.C. Ramamurthy, G. Madras, Morphology controllable microwave absorption property of polyvinylbutyral (PVB)-MnO2 nanocomposites. *Compos. Part B Eng.* **2018**, 132, 188–196.
(36) Y. Liu, Z. Chen, Y. Zhang, R. Feng, X. Chen, C. Xiong, L. Dong, Broadband and Lightweight Microwave Absorber Constructed by in Situ Growth of Hierarchical CoFe2O4/Reduced Graphene Oxide Porous Nanocomposites. *ACS Appl. Mater. Interfaces* **2018**, 10, 13860–13868.